

# Properties of the $\Lambda(1520)$ Resonance from High-Precision Electroproduction Data

Y. Qiang,<sup>1,2</sup> Ya.I. Azimov,<sup>3</sup> I.I. Strakovsky,<sup>4</sup> W.J. Briscoe,<sup>4</sup> H. Gao,<sup>1</sup> D.W. Higinbotham,<sup>2</sup> and V.V. Nelyubin<sup>5</sup>

<sup>1</sup>*Department of Physics, Duke University Triangle Universities Nuclear Laboratory, Durham, NC 27708, USA*

<sup>2</sup>*Thomas Jefferson National Accelerator Facility, Newport News, VA 23606, USA*

<sup>3</sup>*Petersburg Nuclear Physics Institute, Gatchina, 188300, Russia*

<sup>4</sup>*Center for Nuclear Studies, Department of Physics, The George Washington University, Washington, DC 20052, USA*

<sup>5</sup>*University of Virginia, Charlottesville, VA 22901, USA*

High-resolution spectrometer measurements of the reaction  $H(e, e'K^+)X$  at small  $Q^2$  are used to extract the mass and width of the  $\Lambda(1520)$ . We investigate the influence of various assumptions used in the extraction. The width appears to be more sensitive to the assumptions than the mass. To reach a width uncertainty about 1 MeV or better, one needs to know the structure of the non-resonant background. Based on the new Jefferson Lab Hall A data, our final values for the Breit-Wigner parameters are  $M = 1520.4 \pm 0.6(\text{stat.}) \pm 1.5(\text{syst.})$  MeV,  $\Gamma = 18.6 \pm 1.9(\text{stat.}) \pm 1(\text{syst.})$  MeV. We also estimate, for the first time, the pole position for this resonance and find that both the pole mass and width seem to be smaller than their Breit-Wigner values.

PACS numbers: 13.30.Eg, 13.60.Rj, 14.20.Jn

## I. INTRODUCTION

The  $\Lambda(1520)$  is considered to be one of the best known baryon resonances. It is, in particular, an excited baryon state of the highest rank (4 stars) in the Review of Particle Physics (RPP) [1]; but its properties are still not exceedingly well understood. For example, its decay properties [1], with a rather large branching ratio to the  $\pi\pi\Lambda$  channel, hint at an unexpectedly strong coupling to the kinematically suppressed channel  $\pi\Sigma(1385)$  that is stronger than to the main decay channels  $\pi\Sigma$  and  $\bar{K}N$ . This could mean that the  $\Lambda(1520)$  has a molecular nature (see, *e.g.*, Ref. [2] and references therein). On the other hand, evidence has arisen [3] that a new, previously unobserved, resonance  $\Sigma(1380)$  with  $J^P = 1/2^-$  and decay to  $\Lambda\pi$  might influence the mode  $\Lambda(1520) \rightarrow \pi\pi\Lambda$ . These examples show that more detailed studies of the  $\Lambda(1520)$ , which may clarify both its nature and the hyperon spectroscopy, are needed.

Surprisingly, the latest experimental inputs in RPP for the mass and width of the  $\Lambda(1520)$  are dated before 1980. Since then, many new experiments have been performed and much more data with the  $\Lambda(1520)$  observed either as the main goal or as a byproduct have been collected (even more data are expected to appear in near future). For example, while the main purpose of the recent Jefferson Lab (JLab) Hall A experiment [4] was to search for  $\Theta^+$ -partners, it also produced high quality data on the  $\Lambda(1520)$ . The preliminary analysis [4] of this data provided results for the mass and width of this resonance that were in reasonable agreement with the RPP values.

Note that most of the earlier high-precision mass and width values, in particular those used for averaging in RPP [1], had come either directly from production measurements with bubble chambers, or indirectly from partial wave analyses. High-energy spectrometers did not have high enough resolution for such measurements, and thus, their results could not compete with bubble chamber data, even when collecting much

higher statistics. Now, the High Resolution Spectrometers (HRS's) [5] in the Hall A provided an exciting accuracy ( $\sigma = 1.5$  MeV [4]), comparable to the best previous resolutions. That is why we reconsider here the Hall A data with the aim to analyze the  $\Lambda(1520)$  more accurately.

In this Letter, of course, we will not be able to answer all questions related to the  $\Lambda(1520)$ . We are going to extract new values of its basic parameters, mass and width. But, in addition to this standard procedure, we try also to investigate how reliable may be those values, how strongly they can depend on various assumptions used. One more new point in this Letter is extraction of the pole position for the  $\Lambda(1520)$ .

## II. JLAB HALL A EXPERIMENT

High-resolution measurements of the missing mass (MM) spectra were developed at near-forward production angles in the reactions  $ep \rightarrow e'K^\pm X$  and  $e'\pi^+ X$ . The experiment [4] took place in Hall A at the Thomas Jefferson National Accelerator Facility (JLab) using a 5.09 GeV electron beam incident on a 15 cm liquid hydrogen target. Scattered electrons were detected in one of the HRS's in coincidence with electroproduced hadrons in the second HRS. Each spectrometer was positioned at  $12.5^\circ$  relative to the beamline, but the use of additional septum magnets [6] allowed to reach smaller production angles, down to  $\sim 6^\circ$ . In this configuration, the spectrometers have an effective acceptance of approximately 4 msr in solid angle and  $\pm 4.5\%$  in momentum, while still maintaining their nominal  $10^{-4}$  full-width half-max momentum resolution [5]. To obtain the desired MM coverage, the central momentum of the electron HRS was varied between 1.85 and 2.00 GeV, while the central momentum of the hadron HRS was changed between 1.89 and 2.10 GeV. In such configuration, the average momentum transfer of the virtual photon was

$\langle Q^2 \rangle \approx 0.1 \text{ (GeV/c)}^2$ , and the average center-of-mass (CM) photon energy was  $\langle E_{\gamma^*}^{\text{cm}} \rangle = 1.1 \text{ GeV}$  which means that  $\langle W \rangle = 2.53 \text{ GeV}$ . For the kaon kinematics, the CM scattering angle was  $5.6^\circ \leq \theta_{\gamma^* K}^{\text{cm}} \leq 11.4^\circ$ , and the angular acceptance was  $\Delta\Omega_{\gamma^* K}^{\text{cm}} \approx 38 \text{ msr}$ .

Calibration of HRS's was based on precise measurements of the known MM peaks for the neutron (in  $\pi^+ X$ ) and for the hyperons  $\Lambda(1116)$ ,  $\Sigma^0(1193)$  (both in  $K^+ X$ ). These three baryons decay through weak interactions, and the proper widths of their peaks are negligible. Therefore, the observed widths of the peaks directly determine the MM resolutions at the corresponding momenta of the registered meson ( $\pi^+$  or  $K^+$ ). Then, the resolution of HRS for the  $\Lambda(1520)$  may be determined by extrapolation of those resolution values to the MM region of 1520 MeV. Such a procedure gave the resolution  $\sigma = 1.5 \text{ MeV}$  [4]. We apply this resolution when fitting the data.

Positions of the peaks, as measured by the HRS, show deviations from the RPP mass values, different for different peaks (see Fig. 1). We use those shifts to correct the spectrometer MM scale at the corresponding mass value. Then, mass correction for the peak of  $\Lambda(1520)$  may be obtained by extrapolation of the peak shifts to the MM region of 1520 MeV. As seen in Fig. 1, the measured shift values admit simple linear extrapolation providing negligible correction near 1520 MeV.

Let us estimate uncertainty of this zero correction for the mass scale near  $\Lambda(1520)$ . The same peak positions, being measured in 4 different parts of the HRS, show some spread of the mass values. It contributes, of course, to systematic uncertainty of any mass measurement by the HRS, but appears to be small, less than 0.2 MeV, *i.e.*, smaller than the statistical errors shown by error bars in Fig. 1.

More essential for the mass scale beyond location of the three peaks is another source of uncertainty, related to the extrapolation procedure. Statistical errors of the particular shifts (mainly of hyperon ones) in Fig. 1 spreads the possible slope for the linear extrapolation. As a result, the MM scale correction near 1520 MeV may be non-zero, having uncertainty about  $\pm 1.5 \text{ MeV}$ . We will consider this value as the possible systematic uncertainty for the position of the  $\Lambda(1520)$ . Further experimental details can be found in Refs. [4, 7].

### III. CURRENT PARAMETERS OF THE $\Lambda(1520)$

Before we proceed further with our analysis, let us briefly consider earlier results (Table I) that were used in the RPP averaging [1]. The different values for the mass and width of the  $\Lambda(1520)$  look to be in reasonable agreement with each other and with the current average.

The corresponding works fit the data by accounting for both the resonance itself and a background. However, they use different approaches to this task. Most papers deal with the resonance production [8–11]. They study

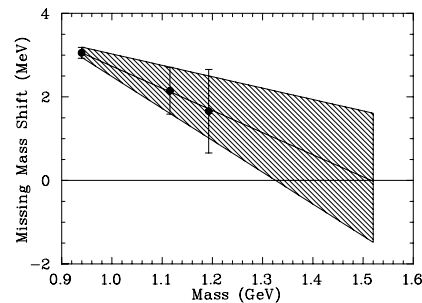


FIG. 1: Mass calibration using the missing mass measurements of the neutron,  $\Lambda(1116)$ , and  $\Sigma^0(1193)$ . The vertical axis shows deviation of the measured mass from the RPP mass value [1] given at the horizontal axis. The linear best-fit result (the central solid line) is extrapolated to the  $\Lambda(1520)$  position. The hatched area characterizes possible errors of the extrapolated correction to the scale calibration.

TABLE I:  $\Lambda(1520)D_{03}$  parameters.

Mass (MeV)	Width (MeV)	Evts	Year	Ref.
$1517.3 \pm 1.5$	$16.3 \pm 3.3$	300	1980	[8]
$1517.8 \pm 1.2$	$14 \pm 3$	5k/677	1979	[9]
$1519.7 \pm 0.3$	$16.3 \pm 0.5$	4k	1977	[10]
$1519.4 \pm 0.3$	$15.5 \pm 1.6$	2k	1975	[11]
$1520.0 \pm 0.5$	$15.4 \pm 0.5$	PWA	1978	[12]
$1519 \pm 1$	$15.0 \pm 0.5$	PWA	1977	[13]
avr. $1519.5 \pm 1.0$	avr. $15.6 \pm 1.0$		2008	[1]

various inelastic reactions, with various many-particle final states, and look for a peak in the mass distribution of one or another final subsystem. The distribution is described by a Breit-Wigner (BW) contribution with some non-coherent (non-interfering) background. Any possible interference with other resonances is neglected as well. Now we consider in some detail the difference in treatments of various production measurements.

Paper [8] considers only the  $K^- p$  decay channel, with the relativistic BW term having the momentum-dependent width and with the background linear in  $M(K^- p)$ . On the other hand, the authors of Ref. [9] obtain the  $\Lambda(1520)$  mass mainly from mass distributions in different decay channels,  $\pi^- \Sigma^+$  and  $\pi^+ \Sigma^-$ , with small addition of  $\Lambda \pi^+ \pi^-$  events. The resonance width is extracted only from the  $\Lambda \pi^+ \pi^-$  events. Here, the BW term is presented in the non-relativistic form, with the energy-independent width; the background is taken to be linear in  $M(\pi \Sigma)$  or  $M(\Lambda \pi^+ \pi^-)$ .

Paper [10] studies several final subsystems, but extracts the best (and final) values for the  $\Lambda(1520)$  mass and width from the  $K^- p$  mass spectra. It uses the relativistic form for the BW term, with the energy-independent width. The background is assumed to be linear in  $M^2(K^- p)$ .

Paper [11] mainly studies also the decay channel  $K^-p$ , the width is assumed to be energy-dependent, accounting for the appropriate angular-momentum barrier. More details of the BW term and, especially, background are not described explicitly.

On the other hand, papers [12, 13] study the direct resonance formation. They construct partial wave analyses for the elastic  $K^-p$  scattering, with some way (different in the two papers) of accounting for inelastic processes. Separation of resonance/background is made in a particular partial amplitude, so their contributions are coherent. Both papers use the non-relativistic BW form and include the angular momentum barrier into the width, though in different ways. The background is also described differently in the two papers.

Without any justification, all those papers, which assume the energy dependent width of the  $\Lambda(1520)$ , describe the total width as having the threshold behavior related only to the  $K^-p$  channel. Meanwhile, different thresholds, corresponding to other decay channels (*e.g.*,  $\pi\Sigma$ ), should also affect the total width.

All the described approaches would be completely equivalent for an ideally narrow resonance. But, for the case of a finite width, such as the  $\Lambda(1520)$ , they should provide different results at some level of accuracy. In what follows, we not only extract the resonance parameters from the Hall A measurements, but also estimate the sensitivity of our results to how the experimental data was treated.

#### IV. PRESENT ANALYSIS OF THE $\Lambda(1520)$

The earlier Hall A paper [4] analyzed the inclusive reactions

$$\gamma^* + p \rightarrow K^+(\pi^+) + X \quad (1)$$

mainly to search for narrow (presumably, exotic) peaks in the missing mass (*i.e.*,  $M_X$ ), with widths  $\sim 1$  MeV or less. Respectively, the experimental data were presented with the narrow binning in  $M_X$ : the width of one bin was 1 MeV. For the case of  $K^+$ , the MM distribution showed, of course, the pronounced peak of the known resonance  $\Lambda(1520)$ . It was analyzed, but only in a preliminary way, to demonstrate reasonable agreement of its mass and width with their RPP values [1] and, thus, to confirm satisfactory understanding of the mass scale and resolution. Here we reanalyze the  $\Lambda(1520)$  more accurately.

First of all, we modify data presentation. The 1 MeV steps for  $M_X$ , used in Ref. [4], were appropriate to scan in searching for resonances of  $\sim 1$  MeV width. But bins of such a size are unsuitable to study the resonance of  $\sim 16$  MeV width with Gaussian resolution 1.5 MeV. Too narrow bins provided stronger fluctuations and excessively large statistical errors for every experimental point. That is why in the present reanalysis of the data for  $\Lambda(1520)$  we increase the bin size from 1 MeV to

4 MeV. This size is more adequate for the resolution with  $\sigma = 1.5$  MeV, it essentially diminishes statistical errors and fluctuations. This is seen in Fig. 2, which displays the cross section  $d\sigma/(dM_X d\Omega_{\gamma^*K})$  as a function of  $M_X$  for two different bin sizes. In what follows, we use the distribution in the lower panel of Fig. 2 to extract the  $\Lambda(1520)$  mass and width.

The system  $X$  in the shown mass region may consist of either  $N\bar{K}$ , or  $\Sigma(\Lambda)$  hyperon, accompanied by pion(s). Any resonance is revealed in the MM distribution inclusively, being summed over all possible final states. The width of  $\Lambda(1520)$  also consists of several contributions from different decay modes. Their energy dependence should be different, which was not accounted for in the preliminary analysis [4], but will be taken into account now. Furthermore, in contrast to all earlier works, we will try various manners of data treatment and consider their influence on the resulting extracted values of the resonance parameters.

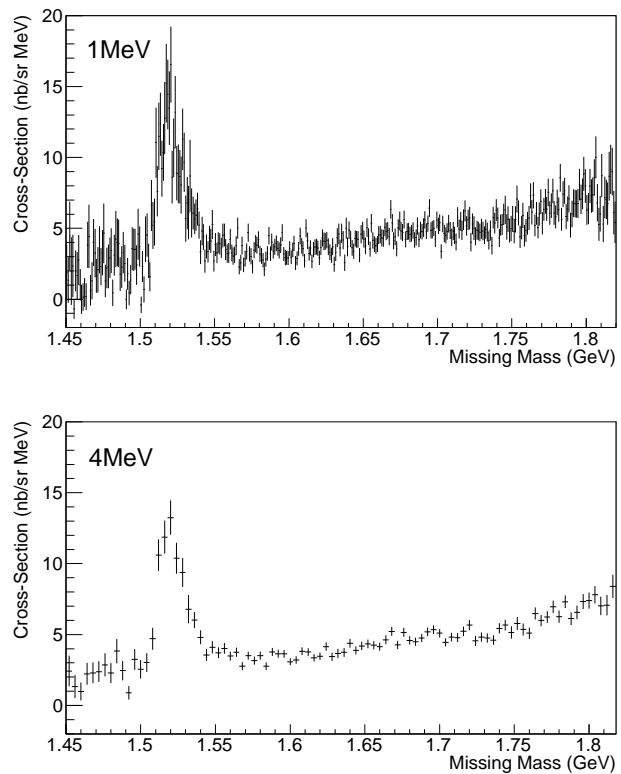


FIG. 2: Missing mass distribution in the reaction  $\gamma^*p \rightarrow K^+X$  [4] with two different binnings: 1 MeV in the upper panel; 4 MeV in the lower panel.

Generally, we describe the MM spectra in the form

$$\text{Fit} = BW + BG, \quad (2)$$

where  $BW$  is the Breit-Wigner contribution for the resonance  $\Lambda(1520)$ , and the term  $BG$  combines all other con-

tributions (including other possible resonances), which provide a background for the  $\Lambda(1520)$ .

The BW contribution may be written as

$$BW = A_{BW} \Gamma(M_X) D(M_X). \quad (3)$$

In the non-relativistic form, we have

$$D_{nr}^{-1}(M_X) = (M_X - M_0)^2 + \Gamma^2(M_X)/4. \quad (4)$$

In the relativistic form, this denominator should look like  $|M_X^2 - [M_0 - i\Gamma(M_X)/2]^2|^2$ , but usually  $\Gamma^2 \ll M_0^2$ , and  $D^{-1}$  may be approximately written in the form

$$D_{rel}^{-1}(M_X) = (M_X^2 - M_0^2)^2 + M_0^2 \Gamma^2(M_X). \quad (5)$$

With the energy-independent width, we define  $\Gamma(M_X) \equiv \Gamma_0$ . Here  $M_0$  and  $\Gamma_0$  may be considered as the BW mass and width of the  $\Lambda(1520)$ . It is definitely so for the non-relativistic form; more detailed discussion of the BW parameters for the relativistic form will be presented in section V.

The energy-dependent width has a more complicated structure. Let us recall that the total width is the sum of partial ones for all decay channels,  $\Gamma = \sum_i \Gamma_i$ . Here we emphasize that every partial width should have its own energy dependence, corresponding to the threshold and kinematical properties of the particular decay channel.

For a two-particle decay of the initial state of mass  $M_X$ , the threshold behavior is proportional to  $p^{1+2l}$ , where  $p$  is the CM momentum of the decay products,  $l$  is their orbital angular momentum. The channels  $\bar{K}N$  and  $\pi\Sigma$  in decays of the resonance  $\Lambda(1520)$  with  $J^P = 3/2^-$  have  $l = 2$ . Therefore, for their partial widths we can write

$$\Gamma_{\bar{K}N}(M_X) = \Gamma_0 B_{\bar{K}N} \left( \frac{p_K}{p_{0K}} \right)^5 \left( \frac{M_0^2}{M_X^2} \right)^2, \quad (6)$$

$$\Gamma_{\pi\Sigma}(M_X) = \Gamma_0 B_{\pi\Sigma} \left( \frac{p_\pi}{p_{0\pi}} \right)^5 \left( \frac{M_0^2}{M_X^2} \right)^2, \quad (7)$$

where  $B_i$  are the branching ratios for the corresponding decay channels,  $p_K$  and  $p_\pi$  are the corresponding momenta in the rest-frame of the mass  $M_X$ , while  $p_0$  are those momenta at  $M_X = M_0$ . The form of the last factors is chosen so to not violate the analyticity of amplitudes in the nearby  $M_X^2$  region and to have a non-increasing ratio  $\Gamma(M_X)/M_X$  even at  $M_X \rightarrow \infty$ .

Three-particle final states are described by several parameters, so they provide more complicated structure to the corresponding partial widths. But the threshold behavior is rather simple, proportional to  $(\sqrt{T})^{4+2L}$ , where  $T$  is the released kinetic energy,  $L$  is the sum of final orbital momenta (the first term in the exponent is due to the 3-particle phase space). To have  $J^P = 3/2^-$ , the system  $\pi\pi\Lambda$  needs at least one  $P$ -wave, so  $4 + 2L = 6$ , and we may write

$$\Gamma_{\pi\pi\Lambda}(M_X) = \Gamma_0 B_{\pi\pi\Lambda} \left( \frac{T(M_X)}{T(M_0)} \right)^3 \left( \frac{M_0^2}{M_X^2} \right), \quad (8)$$

with  $T(M_X) = M_X - M_\Lambda - 2M_\pi$ .

Decays of the  $\Lambda(1520)$  are dominated by only three channels,  $\bar{K}N$ ,  $\pi\Sigma$ , and  $\pi\pi\Lambda$ . Branching ratios for two other channels,  $\pi\pi\Sigma$  and  $\Lambda\gamma$ , are not more than 1% each [1], and we neglect them here. Also neglected is the channel  $\Sigma^0\gamma$ , with an even lower branching ratio [1]. For the main channels we use the branchings

$$B_{\bar{K}N} = 0.46, \quad B_{\pi\Sigma} = 0.43, \quad B_{\pi\pi\Lambda} = 0.11, \quad (9)$$

which agree with the RPP tables [1]. Summing over all decay channels, we have  $\Gamma(M_0) = \Gamma_0$ .

Now we need to describe the background. Here we also discuss various possibilities. First of all, background  $BG$  consists of several terms.

Contribution of the  $S$ -wave  $\bar{K}N$  continuum to the MM spectrum is described by the term

$$BG_N = A_{\bar{K}N} \sqrt{M_X - M_{th}}, \quad M_{th} = M_N + M_K, \quad (10)$$

while  $D$ -wave of this system is contained in the BW term of the  $\Lambda(1520)$  with the energy-dependent width. We neglect the  $P$ - and higher-wave contributions.

The essential hyperon-meson contributions have lower thresholds, and their non-resonance contribution near the  $\Lambda(1520)$  may be approximated by a combination of three simple terms:

$$BG_{Y0} = A_{Y0} = \text{const}, \quad (11)$$

$$BG_{Y1} = A_{Y1} (M_X - M_{th}), \quad (12)$$

$$BG_{Y2} = A_{Y2} (M_X - M_{th})^2. \quad (13)$$

In addition to such smooth contributions, MM spectra in the area of  $M_X \approx 1520$  MeV may also contain contributions of additional resonances, except the presently studied  $\Lambda(1520)$ . First of all, we mean the  $\Lambda(1405)$ , which decays nearly totally into  $\Sigma\pi$  [1]. But in our inclusive measurements with  $M_X > 1.45$  GeV, it cannot be separated from the  $\Sigma(1385)$ , with the dominant decay into  $\Lambda\pi$  and the 10% level for  $\Sigma\pi$  [1]. Moreover, the  $N\bar{K}$  channel may also contain contributions of the two resonances, as sub-threshold ones (through their BW tails). Our data do not separate decay channels, and, after all, we write background from such resonance contributions in the form

$$BG_R = A_R \Gamma_R D_R(M_X), \quad (14)$$

with

$$D_R^{-1} = (M_X^2 - M_R^2)^2 + (M_R \Gamma_R)^2. \quad (15)$$

Here we neglect energy dependence of the width and use parameters of the  $\Lambda(1405)$ :

$$M_R = 1406 \text{ MeV}, \quad \Gamma_R = 50 \text{ MeV},$$

in accordance with the RPP tables [1].

Above the  $\Lambda(1520)$ , the tables of RPP [1] also present several resonances, both  $\Lambda$ - and  $\Sigma$ -like (with different star status). But our MM spectra (Fig. 2) do not show any reliable manifestations of resonances, at least up to  $\sim 1670$  MeV, and we will not take them into account explicitly.

Thus, for extracting the mass and width of the  $\Lambda(1520)$ , we use the MM spectrum shown in the lower panel of Fig. 2 and restrict ourselves to the mass interval from 1.45 GeV to 1.65 GeV (this corresponds to 13,070 detected events). To the peak, we apply the BW term (3), while the background is described by various combinations of terms (10)-(14). In all cases, we use the normalizing coefficients  $A_i$  as free fitting parameters, together with the BW parameters  $M_0$  and  $\Gamma_0$ . Further, for the best-fit procedure, we use two not quite equivalent methods, least-squares (min- $\chi^2$ ) and log-likelihood (LL) ones. In such a way, we obtain several sets of numerical values for pairs ( $M_0$ ,  $\Gamma_0$ ) and can trace their dependence on the assumptions used.

## V. RESULTS AND THEIR DISCUSSIONS

We begin with considering changes of the BW mass  $M_0$ . They appear to be rather small, though not always negligible. The non-relativistic expression (4) for the BW term provides  $M_0$  values lower than the relativistic Eq.(5), at the level of  $\sim 0.05$  MeV.

Similarly, the LL procedure gives lower  $M_0$  than min- $\chi^2$ ; the difference may be as small as 0.01 MeV, but may reach  $\sim 0.15$  MeV. Structure of the background can also shift  $M_0$ ; the difference for various variants which we use is, again, not more than 0.15 MeV.

A more essential effect comes from energy dependence of the width. Description with the energy-dependent width results in  $M_0$  about 0.6 MeV lower than for the energy-independent width. Interestingly, it is at the same level as our statistical uncertainty for  $M_0$ , which is  $\sim 0.6$  MeV in all the studied cases.

Changes of the BW width  $\Gamma_0$  also show some regularities. Shifts of results for using the (non-)relativistic Eqs.(4) or (5) are not more than 0.06 MeV. The LL fitting gives a lower width than min- $\chi^2$ ; the difference may be 0.2 MeV, but may reach  $\sim 0.9$  MeV (for comparison, our statistical uncertainty for the width is  $\sim 2$  MeV).

More complicated is the influence of the background description. By changing different possible combinations of background terms (10)-(13), we change  $\Gamma_0$ , but not very strongly, not more than 0.2 MeV. More influential is the resonance  $\Lambda(1405)$ . Its exclusion diminishes  $\Gamma_0$ ; the difference may be up to  $\sim 1$  MeV (the corresponding shift of  $M_0$  is much smaller, not more than 0.1 MeV).

Now we are able to formulate some conclusions, which may have more general character.

- The width of  $\Lambda(1520)$  is sufficiently small, so the relativistic and non-relativistic forms give practi-

cally the same values of  $M_0$  and  $\Gamma_0$  (at the present level of accuracy).

- By definition, the LL fitting always provides a larger value of  $\chi^2$ , than the min- $\chi^2$  fitting. However, formally they should be equivalent at asymptotically high statistics. In this sense, the present statistics is not asymptotical yet. Both  $M_0$  and  $\Gamma_0$  are different in the two fittings, the differences are comparable to the statistical uncertainties of those BW parameters. In terms of  $\chi^2$  per degree of freedom,  $\chi^2/\text{dof}$ , which is typically  $\sim 1.5$  in our studies here, the LL fitting is up to 0.05 higher than min- $\chi^2$ .
- The  $M_0$  has a smaller statistical uncertainty and is less affected by any change of fitting procedure than the  $\Gamma_0$ .

The last point may be understood as follows. The spectrum in the lower panel of Fig. 2 shows the clear peak for  $\Lambda(1520)$ , and the value of  $M_0$  is mainly determined by the position of the peak maximum, with rather small statistical uncertainty  $\Delta M_0$ . Therefore, any change of the fitting procedure may provide a shift of the  $M_0$  not larger than the  $\Delta M_0$ .

This is not quite similar for the case of width. If neglecting energy dependence,  $\Gamma_0$  is the full width of the peak at its half-height. In terms more directly related to the inclusive MM spectrum, the peak half-height can be formulated as the half-depth from the peak maximum. Thus, though the flanks of the peak are rather well-determined, to extract  $\Gamma_0$  one needs to know the necessary depth, or the proper height of the peak, for the given experimental spectrum. Of course, it essentially depends on the height of the background under the peak. As a result, both statistical uncertainty  $\Delta\Gamma_0$  and changes of  $\Gamma_0$  with fitting changes should be larger than those of  $M_0$ . Moreover, we can admit that changes of  $\Gamma_0$ , with changes of fitting procedure, might exceed the  $\Delta\Gamma_0$  (though this is not the case in our present study).

It is interesting that a change of the mass interval used for fitting may also change the height of the background and, hence, the  $\Gamma_0$ . If we take the smaller interval 1.45–1.60 GeV for our fits, the value of  $M_0$  may shift, but in all cases less than 0.05 MeV, while the value of  $\Gamma_0$  diminishes with a stronger shift, up to  $\sim 0.5$  MeV.

For extracting our resulting BW parameters, we use the BW relativistic expression (3),(5) with energy-dependent width (both points are theoretically motivated to be more reasonable). As a simple, but typical representation for the background, we combine the terms (11), (12) and (14), (15). The corresponding least-squares (min- $\chi^2$ ) fit in the mass interval 1.45 – 1.65 GeV is shown in Fig. 3, together with all separate contributions. This fit corresponds to  $\chi^2/\text{dof}=1.46$  and gives

$$M_0 = 1520.4 \pm 0.6 \text{ MeV}, \quad \Gamma_0 = 18.6 \pm 1.9 \text{ MeV}, \quad (16)$$

with pure statistical uncertainties. Each of the two BW parameters has also a systematic uncertainty. It is about

1.5 MeV, mainly due to the mass scale uncertainty, for  $M_0$ , and about 1 MeV, mainly due to the fitting procedure ambiguity, for  $\Gamma_0$ .

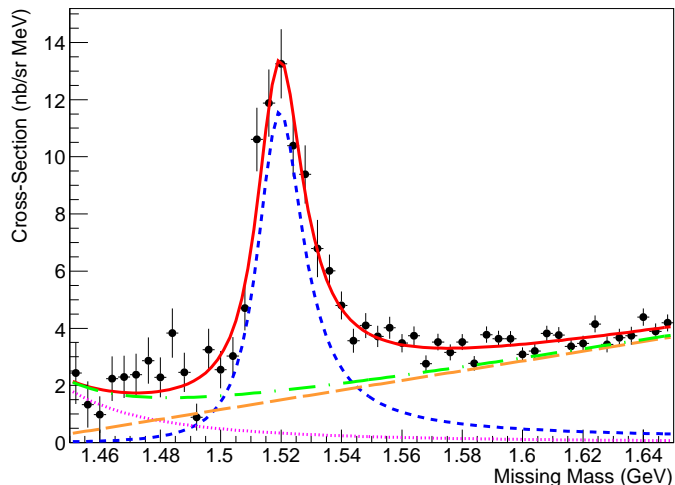


FIG. 3: (Color on line) Fit to the experimental MM distribution (the lower panel of Fig. (2)) is shown by the solid line. The short-dashed line is the BW contribution for the  $\Lambda(1520)$  (note an asymmetric form, due to the energy-dependent width). The total background (dot-dashed line) is the sum of the linear binomial long-dashed line) and tail of the  $\Lambda(1405)$  (dotted line).

For comparison, the same description with the LL fit gives slightly lower values

$$M_0 = 1520.3 \pm 0.6 \text{ MeV}, \quad \Gamma_0 = 17.8 \pm 1.9 \text{ MeV}, \quad (17)$$

and the higher value  $\chi^2/\text{dof}=1.50$ . This LL fit agrees with the values  $M_0 = 1519.9 \pm 0.6 \text{ MeV}$  and  $\Gamma_0 = 16.5 \pm 1.7 \text{ MeV}$  of the preliminary analysis [4] which also used the LL fitting (its systematic uncertainty was estimated to be 3 MeV for the mass; no estimations for the width). The difference between the present and preliminary LL fits is essentially related to excessive fluctuations and statistical errors of the experimental points with 1 MeV binning.

Even without accounting for the systematic uncertainty, both  $M_0$  and  $\Gamma_0$  are in reasonable agreement with previous experimental values and with their RPP average (see Table I). It is worth to note, however, that the uncertainties in the later works [8] and [9] are larger than those in all the earlier works. This may hint that the uncertainties stated in the earlier works (and, therefore, in the average) are too optimistic.

In respect to experimental points, the fit in Fig. 3 looks reasonably good. One can note, however, some small but regular excess of the experimental values over the fit near  $M_X = 1.48 \text{ GeV}$ . It could be due to a small contribution of  $\Sigma(1480)$ , not accounted for in our fit. This contradictory state, with low (one-star) status in the RPP [1],

recently obtained new experimental support [14]. Manifestations of the  $\Sigma(1480)$  seem to be seen also in several other recent papers [15–18]. We have tried to include this resonance into our fit, coherently or incoherently, but large uncertainties prevent us from any conclusions.

Now we can discuss position of the  $S$ -matrix pole corresponding to the  $\Lambda(1520)$ , that has never been discussed for hyperons. It is determined by vanishing of the denominator (5), *i.e.*, by a solution of the equation

$$(W_p^2 - M_0^2)^2 + M_0^2 \Gamma^2(W_p) = 0. \quad (18)$$

This non-linear equation may have non-unique solutions. Physically reasonable is only one of them, close to  $(M_0 - i\Gamma_0/2)$ . It is convenient, therefore, to rewrite Eq.(18) in the form

$$W_p = M_0 [1 - i\Gamma(W_p)/M_0]^{1/2}. \quad (19)$$

Its complex solution gives the pole mass  $M_p = \text{Re } W_p$  and the pole width  $\Gamma_p = -2 \text{Im } W_p$ .

For the energy-independent case  $\Gamma(W) \equiv \Gamma_0$ , the arising  $W_p$  value (19) provides exact BW parameters. Up to corrections of the relative order  $(\Gamma_0/M_0)^2$ , more exact values for the BW mass and width are

$$M_{BW} = M_0 [1 + \frac{1}{8} (\Gamma_0/M_0)^2]; \quad (20)$$

$$\Gamma_{BW} = \Gamma_0 [1 - \frac{1}{8} (\Gamma_0/M_0)^2]. \quad (21)$$

The differences between  $M_{BW}$  and  $M_0$ ,  $\Gamma_{BW}$  and  $\Gamma_0$  arise due to the approximate character of expression (5). The corresponding shifts are numerically small, much smaller than the statistical uncertainties (16).

If we assume the width to be energy-dependent and take it as the sum of expressions (6), (7), and (8), then, by definition,  $\Gamma(M_0) = \Gamma_0$ . Of course, the solution of Eq.(19) still corresponds to the pole position, but it differs from the simple BW position of the energy-independent case. Numerical solution with values (16) for  $M_0$  and  $\Gamma_0$  gives

$$M_p = 1518.8 \text{ MeV}, \quad \Gamma_p = 17.2 \text{ MeV}. \quad (22)$$

Note that  $M_p < M_{BW}$ ,  $\Gamma_p < \Gamma_{BW}$ , with the mass difference exceeding the statistical uncertainty. Such relation for masses may be rather general (model independent), as suggested by comparison with the mass pairs (BW and pole) shown for  $\pi N$  resonances in Listings of RPP [1]. The assumption is also supported, if one solves Eq.(19) by decomposing in degrees of  $\Gamma_0/M_0$ . In this way we obtain

$$M_p - M_{BW} = -\frac{1}{4} M_0 (\Gamma_0/M_0) \Gamma'_0; \quad (23)$$

$$\Gamma_p - \Gamma_{BW} = \frac{1}{8} \Gamma_0 (\Gamma_0/M_0) (3\Gamma'_0 - M_0 \Gamma''_0). \quad (24)$$

Here  $\Gamma_0 = \Gamma(M_0)$ , while  $\Gamma'_0 \equiv d\Gamma(M_X)/dM_X$ ,  $\Gamma''_0 \equiv d^2\Gamma(M_X)/(dM_X)^2$  taken at  $M_X = M_0$ . Note that parametrically both  $\Gamma'_0$  and  $\Gamma''_0$  are proportional to  $\Gamma_0$ . The three quantities  $\Gamma_0/M_0$ ,  $\Gamma'_0$ , and  $M_0\Gamma''_0$  are dimensionless and, thus, have the same order of smallness, though may be very different numerically.

If  $M_0$  is not far from threshold of a decay channel, the  $\Gamma(M_X)$  is an increasing function near  $M_0$ , and  $\Gamma'_0 > 0$ , providing  $M_p < M_{BW}$ . Relation for the widths is less definite. Due to the presence of both the first and second derivatives, the sign of  $\Gamma_p - \Gamma_{BW}$  may depend on more details of the threshold behavior, which can be affected by both the spin of the decaying resonance and by properties of the final state. For the  $\Lambda(1520)$ , all three main contributions (6), (7), and (8) lead to  $\Gamma_p < \Gamma_{BW}$ , in accordance with our numerical solution. It could be different for the case of  $S$ -wave two-particle decays.

In summary, we have found the mass and width of the  $\Lambda(1520)$  in near-forward electroproduction. The extracted Breit-Wigner parameters of the resonance are shown to depend not only on experimental data, but also on the way of treatment of the data. The extracted width is more sensitive to the various treatments than the mass. For the  $\Lambda(1520)$ , the non-resonance background should be accurately studied and understood if one intends to

extract the mass and, especially, width with uncertainty of order 1–2 MeV.

Having the BW mass and width (16), we also give the first estimate (22) of the pole parameters for the  $\Lambda(1520)$ . The pole values for both mass and width tend to be lower than the BW values.

In this Letter we have studied precision reachable for the basic parameters of the  $\Lambda(1520)$ . However, we could not, of course, advance here understanding of many questions related to this resonance. Therefore, we urge its further investigations.

### Acknowledgments

The authors express their gratitude to R. Arndt and to E. Pasyuk for useful discussions. One of the authors (Ya. A.) highly appreciates the hospitality and support extended to him by the George Washington University and by the Jefferson Lab. This work was supported in part by the U. S. Department of Energy under Grants DE-FG02-99ER41110 and DE-FG02-03ER41231, by the Russian State grant SS-3628.2008.2, and by Jefferson Science Associates which operates the Thomas Jefferson National Accelerator Facility under DOE contract DE-AC05-06OR23177.

- 
- [1] C. Amsler *et al.*, (Particle Data Group), Phys. Lett. B **667**, 1 (2008) and 2009 partial update for the 2010 edition.
- [2] L.S. Geng, E. Oset, and B.S. Zou, Eur. Phys. J. **A 38**, 239 (2008); arXiv:0807.4798 [hep-ph].
- [3] J.J. Wu, S. Dulat, and B.S. Zou, arXiv:0909.1380 [hep-ph].
- [4] Y. Qiang *et al.* (JLab Hall A Collaboration), Phys. Rev. **C 75**, 055208 (2007); arXiv:hep-ex/0609025.
- [5] J. Alcorn *et al.*, Nucl. Instrum. Methods **A 522**, 294 (2004).
- [6] P. Brindza *et al.*, IEEE Trans Appl. Supercond. **11**, 1594 (2001).
- [7] Y. Qiang, Ph.D Thesis, MIT, 2007.
- [8] D.P. Barber *et al.* (LAMP2 Group), Z. Phys. **C 7**, 17 (1980).
- [9] S.J.M. Barlag *et al.* (Amsterdam-CERN-Nijmegen-Oxford Collaboration), Nucl. Phys. **B 149**, 220 (1979).
- [10] W. Cameron *et al.* (Rutherford Laboratory- Imperial College Collaboration), Nucl. Phys. **B 131**, 399 (1977).
- [11] M.J. Corden *et al.*, Nucl. Phys. **B 84**, 306 (1975).
- [12] M. Alston-Garnjost *et al.*, Phys. Rev. **D 18**, 182 (1978).
- [13] G.P. Gopal *et al.* (Rutherford Laboratory- Imperial College Collaboration), Nucl. Phys. **B 119**, 362 (1977).
- [14] I. Zychor *et al.*, Phys. Rev. Lett. **96**, 012002 (2006); arXiv:nucl-ex/0506014.
- [15] A. Airapetian *et al.* (HERMES Collaboration), Phys. Lett. **B 585**, 213 (2004); arXiv:hep-ex/0312044.
- [16] A. Aleev *et al.* (SVD Collaboration), Yad. Fiz. **68**, 1012 (2005) [Phys. At. Nucl. **68**, 974 (2005)]; arXiv:hep-ex/0401024.
- [17] S. Chekanov *et al.* (ZEUS Collaboration), Phys. Lett. **B 591**, 7 (2004); arXiv:hep-ex/0403051.
- [18] A. Aleev *et al.* (SVD Collaboration), arXiv:0803.3313 [hep-ex].